



Comparisons of high latitude $E > 20$ MeV proton geomagnetic cutoff observations with predictions of the SEPTR model

S. Kahler, A. Ling

► To cite this version:

S. Kahler, A. Ling. Comparisons of high latitude $E > 20$ MeV proton geomagnetic cutoff observations with predictions of the SEPTR model. *Annales Geophysicae*, 2002, 20 (7), pp.997-1005. hal-00317080

HAL Id: hal-00317080

<https://hal.science/hal-00317080>

Submitted on 1 Jan 2002

HAL is a multi-disciplinary open access archive for the deposit and dissemination of scientific research documents, whether they are published or not. The documents may come from teaching and research institutions in France or abroad, or from public or private research centers.

L'archive ouverte pluridisciplinaire **HAL**, est destinée au dépôt et à la diffusion de documents scientifiques de niveau recherche, publiés ou non, émanant des établissements d'enseignement et de recherche français ou étrangers, des laboratoires publics ou privés.

Comparisons of high latitude $E > 20$ MeV proton geomagnetic cutoff observations with predictions of the SEPTR model

S. Kahler¹ and A. Ling²

¹Air Force Research Laboratory, Space Vehicles Directorate, Hanscom Air Force Base, Massachusetts 01731, USA

²Radex Corporation, 3 Preston Court, Bedford, Massachusetts 01730, USA

Received: 9 October 2001 – Revised: 8 March 2002 – Accepted: 11 March 2002

Abstract. Radiation effects from solar energetic proton (SEP) events are a concern when the International Space Station reaches high latitudes accessible to SEPs. We use data from the 20–29 and 29–64 MeV proton channels of the Proton/Electron Telescope on the SAMPEX satellite during nine large SEP events to determine the experimental geographic cutoff latitudes for the two energy ranges. These are compared with calculated cutoff latitudes based on a computer model, SEPTR (solar energetic particle tracer). The observed cutoff latitudes are systematically equatorward of the latitudes calculated by the SEPTR program using a Tsyanenko field model, but that model produces mean values of $\sim 2^\circ$ for latitudinal differences with observations, ΔLat , which are ~ 3 times smaller than those using the 1995 International Geomagnetic Reference Field model alone. The number distributions of ΔLat are peaked near 0° and decline toward higher values. With the Tsyanenko model, we find no significant trend in either the ΔLat or their variances with increasing K_p .

Key words. Interplanetary physics (energetic particles) – Magnetospheric physics (polar cap phenomena) – Space plasma physics (charged particle motion and acceleration)

1 Introduction

1.1 Radiation and the International Space Station

Space radiation is now recognized as a serious hazard for satellite operations, communications, and human space flights (White and Averner, 2001). With the construction of the International Space Station (ISS), the vulnerability of the human crews on the ISS to the effects of solar energetic proton (SEP) events has become an important concern (Turner, 2001). A recent report by the U.S. National Research Council (Siscoe et al., 2000) focused on radiation risk

management during the ISS construction and concluded that the probability of a significant high-latitude SEP event during an ISS construction flight is nearly unity. The report recommended the development of models to specify the intensity of SEPs and the geographical zones accessible to them. In particular, it urged the development of methods to map latitudinal cutoffs for SEPs at the altitudes of the ISS. Another recommendation was to extend the range of SEP predictions from the present ≥ 10 MeV range to several steps in the biologically effective energy range of 10 to 100 MeV.

The ISS orbit was originally planned for a low-altitude, low-inclination orbit of 28.5° , but with the 1993 agreement to include Russian launch capabilities in the ISS program, it was necessary to increase the orbital inclination to 51.6° to the equator, placing parts of its orbit in high-latitude regions accessible to SEPs. In addition, the construction schedule was roughly in phase with the solar activity cycle, suggesting an enhanced probability of exposure of astronauts to SEPs. Table 1 compares the chronology of the ISS flights with the occurrence of large SEP events listed by the NOAA Space Environment Center at the web address <http://umbra.nascom.nasa.gov/SEP/seps.html>. Proton intensities are integral 5-min averages for energies $E > 10$ MeV, given in particle flux units (pfu), where $1 \text{ pfu} = 1 \text{ p cm}^{-2} \text{ sr}^{-1} \text{ s}^{-1}$, measured by GOES spacecraft at geosynchronous orbit. We give the peak dates of the largest (> 100 pfu) SEP events since the first flight of the ISS construction program in November 1998.

At the time of writing, 17 of the ≥ 40 flights on the NASA manifest for the ISS construction have occurred. One recent flight, the STS-100, from 19 April to 1 May 2001, occurred just after two intense SEP events on 15 and 18 April, although the intensity had fallen to < 20 pfu at the time of the launch and continued to decline during the mission. However, a significant earlier SEP event occurred with a peak in the middle of the STS 106 mission in September 2000. A six-hour extravehicular activity (EVA) on STS 106 took place on 11 September, one day before the SEP event onset. These events have already confirmed the prediction (Siscoe

Correspondence to: S. Kahler
(stephen.kahler@hanscom.af.mil)

Table 1. ISS flights and SEP events

No.	Vehicle	Launch Date ^a	Landing Date ^b	SEP Peak	Intensity (pfu)	Max K_p /date
1	Proton Rocket	20/11/98				
2	STS 88	04/12/98	15/12/98			
3	STS 96	27/05/99	06/06/99			
4	STS 101	19/05/00	29/05/00			
5	Proton Rocket	12/07/00	26/07/00			
6	STS 106	08/09/00	20/09/00	13/09/00	320	7/17, 18
7	STS 92	11/10/00	24/10/00			
8	Soyuz Rocket	31/10/00				
	Expedition 1 crew	02/11/00		09/11/00 26/11/00	14800 942	6/10 7/29
9	STS 97	30/11/00	11/12/00			
10	STS 98	07/02/01	20/02/01			
11	STS 102	08/03/01	21/03/01			
	Expedition 1 crew		18/03/01			
	Expedition 2 crew	09/03/00		03/04/01 11/04/01 15/04/01	1110 355 951	5/04, 05 8/11 7/18
12	STS 100	19/04/01	01/05/01	18/04/01	321	7/18
13	STS 104	12/07/01	24/07/01			
14	STS 105	10/08/01	22/08/01	16/08/01	493	6/17
	Expedition 2 crew		20/08/01			
	Expedition 3 crew	12/08/01				
15	Soyuz Rocket	14/09/01	16/09/01			
				25/09/01 02/10/01	12900 2360	6/25 7/03
16	Soyuz Rocket	21/10/01	23/10/01			
				06/11/01 24/11/01	31700 18900	8/06 9/24
17	STS 108	05/12/01	17/12/01			
	Expedition 3 crew		07/12/01			
	Expedition 4 crew	07/12/01				
				26/12/01 31/12/01	779 108	3/26, 27 4/31

^a ISS occupation start dates for crews^b ISS occupation end dates for crews or rocket docking dates

et al., 2000) that at least two of the planned ISS construction flights would overlap a significant SEP event. Even after the completion of the construction phase, one or two EVAs per month are expected to occur over the life of the ISS. Note that the ISS has been occupied by human crews continuously since November 2000.

The ISS radiation problem is compounded by the statistical tendency for fast CME-driven shocks associated with the SEP events also to produce periods of enhanced geomagnetic activity (Shea et al., 1999) when they impact the Earth. The resulting polar impact zones of SEPs tend to increase with increasing SEP intensities (Shea et al., 1999), especially when $E > 10$ MeV intensities exceed 100 pfu. In Table 1 we show the peak value of K_p , the planetary index of geomagnetic activity, which occurred during the times of the SEP events. K_p values range from 0, the least disturbed, to 9, the most disturbed, with $3 \leq K_p \leq 5$ considered moderately disturbed.

Most peak K_p values of the SEP events of Table 1 are in the very disturbed ($K_p \geq 6$) range, which occurred only 2% of the time during solar cycle 22 (Shea et al., 1999).

1.2 SEP geomagnetic cutoff models

The problem of calculating trajectories of charged particles in the geomagnetic field was first modeled with dipole magnetic fields in the 1930s by Störmer (1955). The basic particle parameter is the rigidity R , defined as the particle momentum divided by its charge. An important parameter of the calculations is the cutoff rigidity R_{cutoff} , the minimum magnetic rigidity of a charged particle that can reach a given point in space from infinity with a given direction of arrival. See reviews by Hoffman and Sauer (1968) and Smart et al. (2000) for early and very recent efforts, respectively, to determine R_{cutoff} for the geomagnetic field. R_{cutoff} is calculated for a given point in space by integrating the equations of mo-

tion for an oppositely charged particle moving away from the point in space. The trajectory of an approaching proton is, therefore, calculated in reverse, and the calculation is done for protons over a range of rigidities. Each trajectory either goes to infinity or some specified distance from the Earth, collides with the Earth, or spends an indeterminately long time trapped in the model geomagnetic field. The first group of trajectories are those of the allowed rigidities ($R > R_{\text{cutoff}}$), and those of the latter two are the forbidden rigidities. The presence of trajectories which collide with the solid Earth provides a complication by producing a penumbra of bands of alternating allowed and forbidden rigidities above R_{cutoff} , with R_L as the lower cutoff rigidity below which all rigidities are forbidden, and R_U as the upper cutoff rigidity above which all rigidities are allowed (e.g. Smart et al., 2000). An effective cutoff rigidity in a given direction, R_C , is determined by either linear averaging of the allowed bands in the penumbra (Shea et al., 1965) or by functions weighted for the particle spectrum and/or detector response (Cooke et al., 1991).

A proton detector at a point in space will have a finite view angle, so the range of directions from which protons can arrive in the detector must also be considered in determining the detector cutoff rigidity. Since this can result in a very computer-intensive effort to calculate trajectories for a range of proton rigidities, each over a range of incident angles, for each point in space, trajectories of only limited sets of zenith angles or planes at specific points in geospace have been calculated (Schwartz, 1959; Cooke et al., 1991). Cutoff rigidities are highest in the eastern and lowest in the western directions, but the penumbral structures vary considerably with change in incident angle. Recent work of Clem et al. (1997) has compared the vertical effective cutoff rigidity, R_C , with an apparent cutoff rigidity, determined by an appropriate averaging over calculated values of R_C extending to 60° off the vertical axis. Working in the 2 to 13 GV range, they found that apparent rigidities generally exceeded vertical R_C by 0.1 to 0.6 GV. If this result holds in the rigidity range of our interest (0.2 to 0.3 GV), then values of R_C based only on vertical cutoff calculations are underestimates of apparent cutoff rigidities.

The geomagnetic field model is a primary factor in the calculation of R_C . The majority of proton magnetospheric trajectory calculations use the International Geomagnetic Reference Field (IGRF) (Langel et al., 1991), which represents the main geomagnetic field, combined with a model of magnetospheric current systems (Flückiger et al., 1991; Boberg et al., 1995; Tsyganenko, 2001). The preferred example of the latter model is that of Tsyganenko (1989; hereafter TSYG89), which includes currents during times of low to moderate ($K_p \leq 5$) geomagnetic disturbances and takes K_p as an input parameter. This system was extended to large geomagnetic disturbances by Boberg et al. (1995). The result of including these current systems reduces the calculated R_C , particularly at high geomagnetic latitudes.

Recent calculations of R_C for vertically incident protons mapped on to a world grid (Smart et al., 2000) have been car-

ried out with a 1990 epoch Definitive IGRF (DGRF90) (Langel, 1992) for altitudes of 20 km (Smart and Shea, 1997a) and 450 km (Smart and Shea, 1997b). The latter calculation, chosen for its application to the ISS, was updated for a 1995 epoch IGRF (Sabaka et al., 1997) and TSYG89 for quiet ($K_p = 0$ and 2) and disturbed ($K_p = 5$ and 5 with a ring current model equivalent of D_{st} index of -300) geomagnetic conditions by Smart et al. (1999a) and (1999b), respectively. The significant reductions in R_C at 450 km with increasing geomagnetic activity, extended to $D_{st} = -500$, were illustrated by Smart et al. (1999c). Since R_C at any geographical location is dependent on local time, all these calculations were averaged for local times of 00:00, 06:00, 12:00, and 18:00 UT.

1.3 Experimental observations of geomagnetic cutoffs

While a particle detector on a satellite with a high-latitude orbit can survey the cutoff latitudes for its particular particle rigidity range, there are several limiting factors to be considered in using such data sets to test computed cutoff models. First, protons in the $10 < E < 100$ MeV range, which is of primary consideration for the ISS (Siscoe et al., 2000), will be enhanced above the background only during times of SEP events. Second, time-intensity profiles from detectors with broad bands of energy response may not show the sharp drops needed for precise determinations of cutoff latitudes. More important, while cutoff calculations are typically done only for vertical cutoffs (e.g. Smart et al., 1999a, b), the finite detector geometries allow for particles from a range of directions to be counted. Since the cutoffs at a given point vary significantly with azimuthal angle (e.g. Clem et al., 1997), the calculated vertical cutoff latitudes may not correspond well to observed cutoff latitudes. A notable exception was the cosmic ray experiment on the HEAO-3 satellite that recorded the energy, charge, and direction of every incident cosmic ray ion. Comparison of those HEAO-3 data with the cutoff predictions verified the principal features of the predictions, but showed that the predicted cutoffs were about 5% higher than those observed (Smart and Shea, 1994). This result was consistent with earlier comparisons, as briefly reviewed by Ogliore et al. (2001). This means that for a given particle rigidity, the observed geomagnetic cutoffs lie equatorward of the calculated values.

Near real-time color-coded displays of global distributions of energetic particle counting rates from the polar-orbiting NOAA POES satellites are currently available at the web site <http://www.sec.noaa.gov/tiger/>. Proton counts from omnidirectional detectors with four energy channels in the range 16–275 MeV are shown plotted on world grids, with $E > 15$ MeV proton counts displayed on geographic polar plots. While not suitable for the measurement of geomagnetic cutoffs R_C we seek here, they allow for a comprehensive view of the zones of SEP precipitation in significant SEP events.

The optimal instruments for determining geomagnetic cutoffs have been the Mass Spectrometer Telescope (MAST) and Proton/Electron Telescope (PET) on the Solar, Anoma-

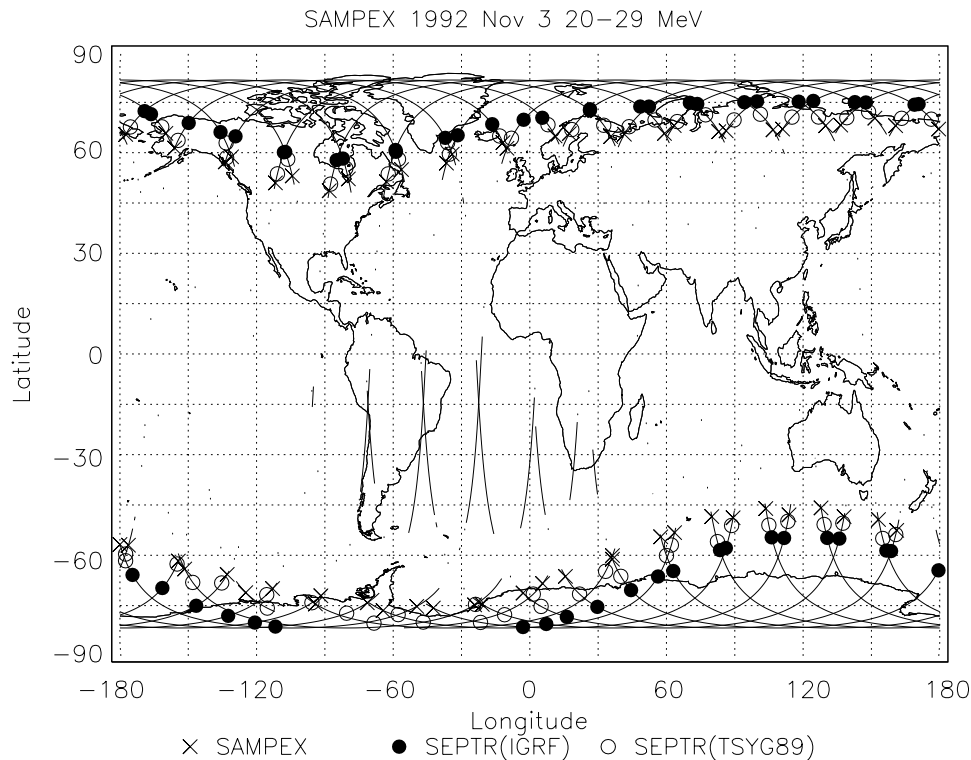


Fig. 1. The world grid for 3 November 1992 showing the observed PET 20–29 MeV proton cutoffs (crosses), the calculated SEPTR Tsyganenko field cutoffs (open circles), and the calculated SEPTR IGRF field cutoffs (solid circles). High-latitude and SAA portions of the SAMPEX orbit are shown. In general, the IGRF cutoffs are poleward of the Tsyganenko cutoffs and further poleward of the PET cutoffs.

lous, and Magnetospheric Particle Explorer (SAMPEX) spacecraft, which was launched into a $520 \text{ km} \times 670 \text{ km}$ 82° inclination orbit in 1992 (Ogliore et al., 2001). In normal operations the MAST and PET instruments are zenith pointing (Leske et al., 2001), so that vertical geomagnetic cutoffs can be determined on each side of each polar passage, or four times per orbit. Recently, Ogliore et al. (2001) determined R_C for cosmic ray nuclei from MAST in the rigidity range $500 < R < 1700 \text{ MV}$. Their particle selection criteria discriminated against SEPs, anomalous cosmic rays, and geomagnetically disturbed times. They plotted their cutoffs as functions of invariant latitude, Λ , defined as the magnetic latitude at which a given ideal dipole field line intersects the Earth's surface, and is related to the McIlwain L parameter by $L = \cos^{-2}(\Lambda)$ (Hoffman and Sauer, 1968; Smart and Shea, 1994). In this coordinate system

$$R_C = \times L^{-2} \text{ GV} = C \times \cos^4(\Lambda) \text{ GV}, \quad (1)$$

where C is a constant, and the blocking effects of the solid Earth are ignored. Ogliore et al. (2001) found a best fit for their cutoffs to be $R_C = 15.062 \times \cos^4(\Lambda) - 0.363 \text{ GV}$, lower than that predicted by the relation $R_C = 14.5 \times \cos^4(\Lambda) \text{ GV}$, which was recommended for vertical cutoffs by Smart and Shea (1994) using the DGRF90. This result means that at high latitudes ($\Lambda > 50^\circ$), a given R_C lies several degrees equatorward of the Smart and Shea (1994) calculation.

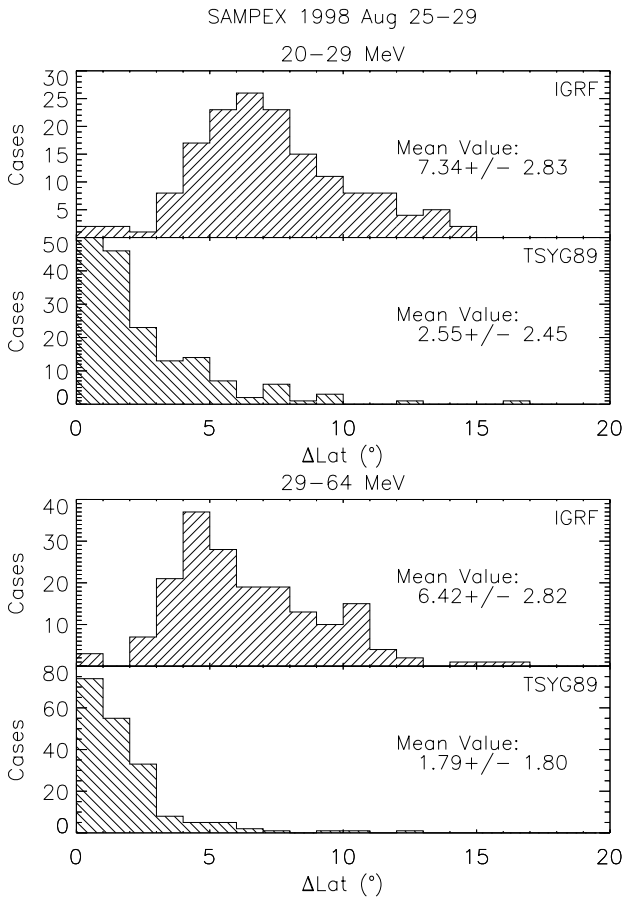
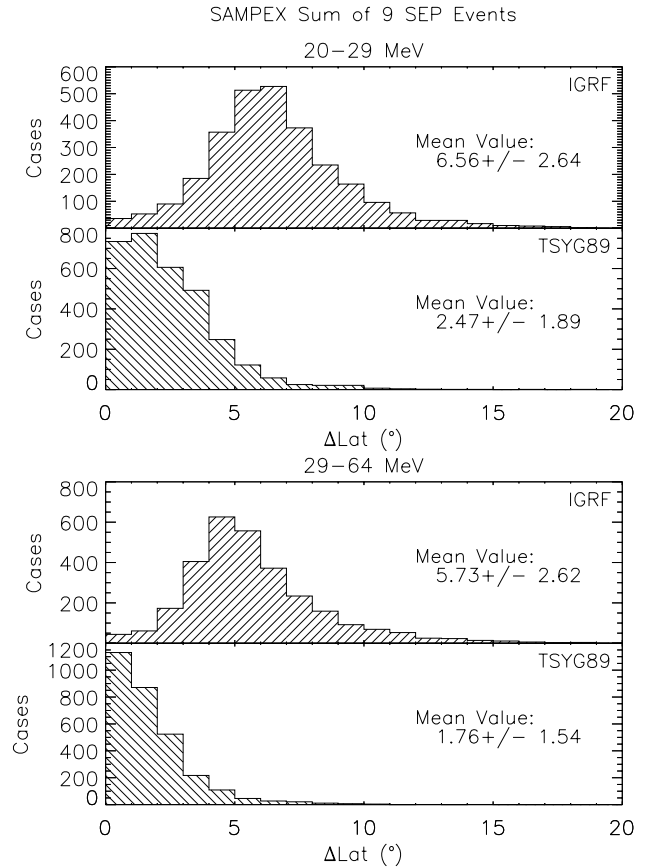
The SAMPEX PET instrument measures protons in the 20–29 MeV and 29–64 MeV energy ranges with a full-width opening angle of 58° (Cook et al., 1993). PET observations were used to determine invariant cutoff latitudes with which SEP ionic charge states could be determined from other SAMPEX instruments (e.g. Oetliker et al., 1997; Mazur et al., 1999). Recently, Leske et al. (2001) have examined PET proton and MAST 8–15 MeV/nucleon He observations to determine the invariant cutoff latitudes, using the DGRF90, for six large SEP events from 1992 to 1998. They found that the cutoff latitudes correlated with the geomagnetic activity parameters K_p and D_{st} , although the correlation could be poor at certain times, such as the onset of a geomagnetic storm. At a given value of K_p or D_{st} the spread in cutoff latitudes was $\sim 2^\circ - 3^\circ$. Correcting for D_{st} effects, they found an invariant cutoff latitude of $\sim 64^\circ$ for MAST observations at $\sim 300 \text{ MV}$. The above Eq. (1) suggested by Smart and Shea (1994), yields an invariant cutoff latitude of 67.7° for $R_C = 300 \text{ MV}$, again several degrees poleward from the observed value.

1.4 The SEPTR programme

The Solar Energetic Particle Tracer (SEPTR) model is based on a Ph.D. thesis of Orloff (1998). SEPTR (Freeman and Orloff, 2001) takes a number of variable input parameters and uses several modifications to the basic particle trajectory

Table 2. Average latitudinal differences ΔLat for the Tsyganenko field in the nine analyzed SEP events

Data Interval	Max K_p	ΔLat 20–29 MeV	ΔLat 29–64 MeV
30/10–06/11/92	6	$2.7^\circ \pm 1.6^\circ$	$1.6^\circ \pm 1.3^\circ$
06/11–10/11/97	7	$3.0^\circ \pm 2.5^\circ$	$2.2^\circ \pm 2.1^\circ$
25/08–29/08/98	8	$2.6^\circ \pm 2.5^\circ$	$1.8^\circ \pm 1.8^\circ$
30/09–02/10/98	5+	$2.4^\circ \pm 2.2^\circ$	$2.1^\circ \pm 1.9^\circ$
12/09–16/09/00	6+	$2.5^\circ \pm 1.8^\circ$	$1.7^\circ \pm 1.6^\circ$
09/11–15/11/00	6+	$1.8^\circ \pm 1.3^\circ$	$1.6^\circ \pm 1.4^\circ$
24/11–29/11/00	7–	$2.9^\circ \pm 1.6^\circ$	$2.0^\circ \pm 1.4^\circ$
30/03–31/03/01	9–	$3.5^\circ \pm 3.1^\circ$	$1.9^\circ \pm 2.1^\circ$
03/04–19/04/01	8+	$2.2^\circ \pm 1.7^\circ$	$1.7^\circ \pm 1.3^\circ$
Average of all events:		$2.5^\circ \pm 1.9^\circ$	$1.8^\circ \pm 1.5^\circ$

**Fig. 2.** Top panels: Histograms of numbers of cases of ΔLat for the 20–29 MeV protons with the IGRF model (top) and Tsyganenko model (bottom). The observing period is 25 to 29 August 1998. Each case is a difference between the calculated (IGRF or Tsyganenko) and observed PET geographic cutoff latitudes. Bottom panel: Same as the above but for the 29–64 MeV protons.**Fig. 3.** Top panels: Histograms of numbers of cases for all nine SEP events of ΔLat for the 20–29 MeV protons with the IGRF model (top) and Tsyganenko model (bottom). Each case is a difference between the calculated (IGRF or Tsyganenko) and observed PET geographic cutoff latitudes. Bottom panel: Same as the above but for the 29–64 MeV protons.

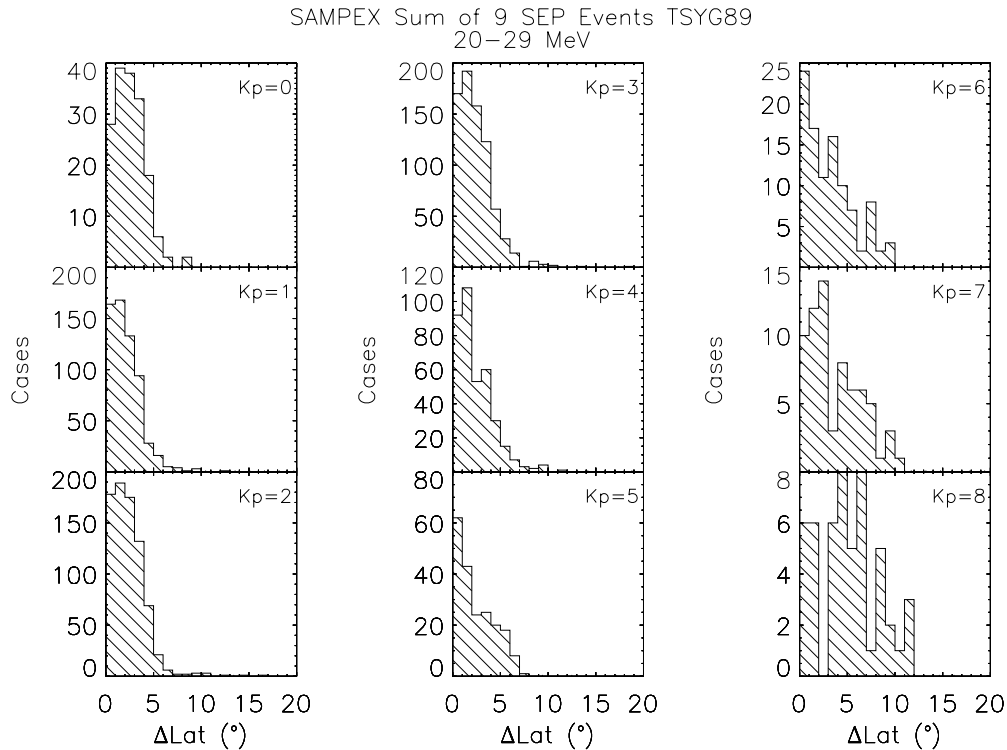


Fig. 4. Histograms of numbers of cases of ΔLat for 20–29 MeV protons and the Tsyganenko model binned by K_p .

calculation described by Smart et al. (2000) to calculate values of R_C at a given location. The model has been validated by several consistency checks and by comparisons of calculated world grids of R_C with those of Smart and Shea (1985) using the same input geomagnetic field models (Freeman and Orloff, 2001).

Although SEPTR was designed to calculate R_C at a specific location, we will use SEPTR to determine whether vertically incident particles of a given rigidity R can reach a given point in space. For the SEPTR input values we use the positions of the SAMPEX spacecraft along its orbit and the rigidities of 0.215 GV and 0.298 GV, corresponding to the mean energies of the 20–29 MeV and 29–64 MeV proton channels of the PET. The trajectories from each point are calculated until: (1) the proton reaches $25 R_E$; (2) the proton trajectory intercepts the solid Earth; (3) the particle travels a distance of $500 R_E$; or (4) the time of proton propagation reaches 1000 time units, where the SEPTR time unit is 0.0212 s. Only trajectories satisfying condition (1) are considered to be allowed. We will use as input field models the 1995 IGRF (Sabaka et al., 1997) and the TSYG89, which is valid for $K_p \leq 5$. When $K_p > 5$, we use the TSYG89 with $K_p = 5$. We do not use here the Boberg et al. (1995) modification to the TSYG89 for $K_p > 5$.

2 Data analysis

We selected for analysis nine SEP events with high $E > 20$ MeV intensities and at least moderate peak values of K_p .

Table 2 gives the selected dates of analysis and the maximum K_p during each period. The first four events were also analyzed by Leske et al. (2001). For each event we determined the geographical cutoff locations for the 20–29 MeV and 29–64 MeV protons of the PET detector. Each cutoff location was taken to be the point at which the rate of change of the PET SEP intensities, measured with 6-second time resolution, was maximum. For each full day of data there were 15 or 16 orbits, so with two cutoff points for each polar pass there were up to 64 cutoff locations per day. All cutoff locations were tabulated and plotted on a world grid for each day, as shown in Fig. 1.

Along each SAMPEX orbit the geographic cutoff locations were calculated with SEPTR for assumed PET proton rigidities of 0.215 and 0.298 GV and a fixed altitude of 600 km, using first the 1995 IGRF (Sabaka et al., 1997) and then the combined 1995 IGRF and TSYG89 reference field. We refer to these fields simply as the IGRF and TSYG89 fields, respectively. The calculated cutoff locations for the two fields were also plotted on the world grids. We found that the calculated cutoff latitudes are almost always poleward of the observed cutoff latitudes, as the example of Fig. 1 shows.

For each orbit we compared the calculated cutoff latitudes of each field model with the observed cutoff latitudes for each PET energy range. For each SEP event we compiled the histograms of numbers of cases versus ΔLat , the difference between the calculated and observed geographic cutoff latitudes, and calculated their mean values and variances. In Fig. 2 we show the distributions for the August 1998 SEP

event. We note first that the IGRF model provides a much worse fit than does the TSYG89 model, by a factor of ~ 3 , for both energy bands. Second, the values of ΔLat are larger for the 20–29 MeV protons than for the 29–64 MeV protons. Third, the distributions are very different for the two models. The IGRF values are peaked near their mean values, while the TSYG89 values are peaked near 0° and decline with increasing ΔLat . The high variances of the latter values are due to the small number of cases of large ΔLat . These properties of the August 1998 event are characteristic of all nine SEP events. In the last two columns of Table 2 we show the means and variances for the TSYG89 model. The bottom row of the table gives the result of summing over all the event orbits, and the histograms are shown in Fig. 3.

We have also compiled histograms of ΔLat as a function of K_p and shown them for the 20–29 MeV protons and the TSYG89 model in Fig. 4. In all of the cases, except where $K_p \geq 7$, the distributions are peaked within 2° of 0° and have the same basic shapes as those of the TSYG89 model of Fig. 3. Figure 5 compares the values of ΔLat as a function of K_p for the IGRF and TSYG89 models. It is not surprising to find that the TSYG89 model is superior to the IGRF model, but we find that the TSYG89 model is nearly independent of K_p . There is a small but insignificant increase in ΔLat for $K_p \geq 6$, above the range for which the TSYG89 model is valid.

Several possible sources of error could contribute to the variances shown in Fig. 5. We pointed out in Sect. 1 that R_{cutoff} at any location is not sharp but rather is characterized by a penumbra over which R_C must be defined. Thus, the imprecise value of R_C might be a source of the variance. However, we have used SEPTR only to calculate whether an interplanetary 0.215 GV or 0.298 GV proton has access to a particular point in the SAMPEX orbit. Since we have very rarely found a SAMPEX polar-cap orbital boundary characterized by any fluctuation in the step function between allowed and forbidden regions, calculated at 6-second intervals, we do not consider this to be a source of the variance.

Another contribution to the variances could be our approximation to the energy ranges of the PET detectors by taking the mean energies, rather than weighting them with an assumed power-law rigidity or energy distribution. If we assume a differential power law in energy E with an exponent $\gamma = -3$, then the mean energies in the two PET channels are 23.3 MeV and 37.4 MeV. These lower mean energies would result in higher, more poleward calculated cutoff latitudes and would increase the values of ΔLat in Table 2. We can use Eq. (1) with $C = 14.5$ to approximate these increases in geographical latitudes L by calculating the changes in invariant latitudes Λ resulting from the corresponding lower values of R_C . For the 20–29 MeV protons Λ increases from 69.55° to 69.68° , an increase of 0.13° and only a small fraction of the average $\Delta\text{Lat} = 2.5^\circ$ shown in Table 2. For the 29–46 MeV protons, however, Λ increases from 67.71° to 68.32° , an increase of 0.6° and a large fraction of the average of $\Delta\text{Lat} = 1.8^\circ$ in Table 2. The resulting increase to $\Delta\text{Lat} = 2.4^\circ$ would make it comparable to that of the 20–29 MeV proton value.

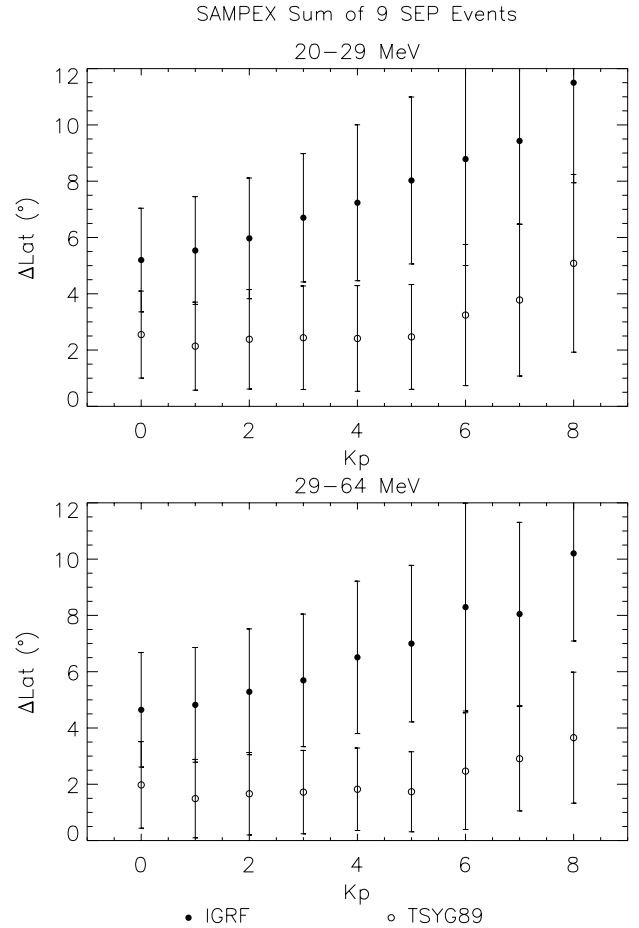


Fig. 5. Top: Comparison of average values of ΔLat for 20–29 MeV protons and for the IGRF model and the Tsyganenko model binned by K_p . Bottom: Same as top except for 29–64 MeV protons.

Cutoff variations with local time may be a minor contribution to the values of ΔLat , but they tend to produce small offsets from the circles of constant Λ , as discussed by Leske et al. (2001). The TSYG89 model that we used incorporates the variations of local time, so they should not be a significant factor in the variances.

Another source of the variances may be the approximation we have made to compare the observed and calculated geographic cutoff latitudes as though they coincided in longitude, when in fact, they lie at different longitudes along the SAMPEX orbit. If contours of constant R_C are inclined to circles of geographic latitude, and the SAMPEX orbit is nearly tangent to those contours, the calculated ΔLat could be larger than that at a fixed longitude. We can estimate the error from this effect by assuming that the geomagnetic dipole is tilted about 11° to the rotational axis, so that the geographic longitudinal gradient of a given Λ should be $\leq 22^\circ/180^\circ$, or $\leq 0.12^\circ$ per degree of longitude. From Fig. 1 we estimate that the geographical longitudinal differences between the observed and calculated cutoffs for a given orbit are $\leq 5^\circ$, so the effective error for a given ΔLat is $\leq 0.6^\circ$.

Note that this effect approaches 0° when the cutoffs lie in the regions of lowest geographic latitudes most important for the ISS. From the symmetry of the orbits we see that the net effect could be negative or positive and hence will increase the widths of the distributions of ΔLat , but not change the resulting average values of ΔLat .

3 Discussion

We have compared the calculated geomagnetic cutoff latitudes of the SEPTR program with the 20–29 and 29–64 MeV proton cutoff latitudes observed with the SAMPEX PET detector for nine SEP events. The TSYG89 model is superior to the IGRF model in providing a significant decrease in ΔLat , as shown in Fig. 5. We found equatorward displacements of $\Delta\text{Lat} = 2.5^\circ$ and 1.8° in the observed cutoffs of 20–29 MeV and 29–64 MeV protons, respectively, similar to those found by other investigators (Ogliore et al., 2001) working in the system of invariant latitudes Λ . However, the number distributions of those displacements are not centered on the mean values, but show declines toward larger values from peaks near $\Delta\text{Lat} = 0^\circ$. This suggests that with the TSYG89 model we have nearly optimum calculated values of geographic cutoff latitudes L , but some other effect, which we cannot identify, is allowing SEPs to reach latitudes lower than calculated in many cases. A strong possibility is that the 3-hour values of K_p are inadequate to characterize the geomagnetic field variations on shorter time scales. If we assume that misleading values of K_p both decrease sharply in number and result in increasing values of ΔLat with increasing size of the misleading values, then we would obtain the kind of distribution shown for the TSYG89 model in Figs. 2, 3, and 4. However, Leske et al. (2001) did not find a significant difference in the correlation between cutoff locations and either K_p or D_{st} , where D_{st} was taken on shorter 1-hour centers.

The invariant cutoff latitudes Λ decrease with increasing K_p at the rate of $\sim 0.9^\circ$ per step in K_p , as shown by Leske et al. (2001) for 8–15 MeV/nucleon He. Since K_p is a measure of disturbed geomagnetic fields, we might expect ΔLat to increase with K_p . However, we found that ΔLat calculated with the Tsyganenko model shows almost no change with increasing K_p , although there is a slight increase in both the mean values and variances of ΔLat when K_p exceeds 5, which is the limit of validity of the Tsyganenko model. Use of the Boberg et al. (1995) extension to the Tsyganenko model, not used here, may decrease those values of ΔLat with higher values of K_p .

Acknowledgements. We thank R. Mewaldt for making the PET data available to us and S. Kanekal for the preliminary processing of the event data. A. Ling acknowledges support from AFRL contract # F19628–00–C–0089. This work was supported in part by AFOSR task 92PL012. Support was also provided by the Defense Threat Reduction Agency under its Integrated Space Modeling development and validation program.

Topical Editor G. Chanteur thanks J. Humble and another referee for their help in evaluating this paper.

References

- Boberg, P. R., Tylka, A. J., Adams, J. H., Jr., Flückiger, E. O., and Kobel, E.: Geomagnetic transmission of solar energetic protons during the geomagnetic disturbances of October 1989, *Geophys. Res. Lett.*, 22, 1133–1136, 1995.
- Clem, J. M., Bieber, J. W., Evenson, P., Hall, D., Humble, J. E., and Duldig, M.: Contribution of obliquely incident particles to neutron monitor counting rate, *J. Geophys. Res.*, 102, 26 919–26 926, 1997.
- Cook, W. R., Cummings, A. C., Cummings, J. R., Garrard, T. L., Kecman, B., Mewaldt, R. A., Selesnick, R. S., Stone, E. C., Baker, D. N., Von Rosenvinge, T. T., Blake, J. B., and Callis, L. B.: PET: a proton/electron telescope for studies of magnetospheric, solar, and galactic particles, *IEEE Trans. Geosci. Remote Sens.*, 31, 565–571, 1993.
- Cooke, D. J., Humble, J. E., Shea, M. A., Smart, D. F., Lund, N., Rasmussen, I. L., Byrnak, B., Goret, P., and Petrou, N.: On cosmic-ray cut-off terminology, *Nuovo Cimento Soc. Ital. Fis. C*, 14, 213–234, 1991.
- Flückiger, E. O., Kobel, E., Smart, D. F., and Shea, M. A.: A new concept for the simulation and visualization of cosmic ray particle transport in the Earth's magnetosphere, *Proc. 22nd Internat. Cosmic Ray Conf.*, 3, 648–651, 1991.
- Freeman, J. W. and Orloff, S.: Specifying geomagnetic cutoffs for solar energetic particles, in: *Space Weather*, (Eds) Song, P., Singer, H. J., and Siscoe, G. L., *Geophysical Monograph*, 125, American Geophysical Union, Washington, D. C., 191–194, 2001.
- Hoffman, D. J. and Sauer, H. H.: Magnetospheric cosmic-ray cut-offs and their variations, *Space Sci. Rev.*, 8, 750–803, 1968.
- Langel, R. A.: IGRF, 1991 Revision, *Eos Trans. AGU*, 73, 182–185, 1992.
- Langel, R., Mundt, W., Barraclough, D. R., Barton, C. E., Golovkov, V. P., Hood, P. J., Lowes, F. J., Peddie, N. W., Qi, G., Quinn, J. M., Shea, M. A., Srivastava, S. P., Winch, D. E., Yukutake, T., and Zidarov, D. P.: International Geomagnetic Reference Field, 1991 revision, *J. Geomag. Geoelectr.*, 43, 1007–1012, 1991.
- Leske, R. A., Mewaldt, R. A., Stone, E. C., and Von Rosenvinge, T. T.: Observations of geomagnetic cutoff variations during solar energetic particle events and implications for the radiation environment at the Space Station, *J. Geophys. Res.*, 106, 30 001–30 011, 2001.
- Mazur, J. E., Mason, G. M., Looper, M. D., Leske, R. A., and Mewaldt, R. A.: Charge states of solar energetic particles using the geomagnetic cutoff technique: SAMPEX measurements in the 6 November 1997 solar particle event, *Geophys. Res. Lett.*, 26, 173–176, 1999.
- Oetliker, M., Klecker, B., Hovestadt, D., Mason, G. M., Mazur, J. E., Leske, R. A., Mewaldt, R. A., Blake, J. B., and Looper, M. D.: The ionic charge of solar energetic particles with energies of 0.3–70 MeV per nucleon, *Astrophys. J.*, 477, 495–501, 1997.
- Ogliore, R. C., Mewaldt, R. A., Leske, R. A., Stone, E. C., and Von Rosenvinge, T. T.: A direct measurement of the geomagnetic cut-off for cosmic rays at Space Station latitudes, *Proc. 27th ICRC*, 10, 4112–4115, 2001.
- Orloff, S.: A computational investigation of solar energetic particle trajectories in model magnetospheres, PhD thesis, Rice University, 1–165, 1998.
- Sabaka, T. J., Langel, R. A., Baldwin, R. T., and Conrad, J. A.: The geomagnetic field, 1900–1995, including the large scale fields

- from magnetospheric sources and NASA candidate models for the 1995 IGRF revision, *J. Geomag. Geoelect.*, 49, 157–206, 1997.
- Schwartz, M.: Penumbra and simple shadow cone of cosmic radiation, *Suppl. Nuovo Cimento*, 11, 27–74, 1959.
- Shea, M. A., Smart, D. F., and McCracken, K. G.: A study of vertical cutoff rigidities using sixth degree simulations of the geomagnetic field, *J. Geophys. Res.*, 70, 4117–4130, 1965.
- Shea, M. A., Smart, D. F., and Siscoe, G.: Statistical distribution of geomagnetic activity levels as a function of solar proton intensity at Earth, 26th ICRC Proc., 7, 390–393, 1999.
- Siscoe, G. L., Carlson, C. W., Carovillano, R. L., Gombosi, T. I., Greenwald, R. A., Karpen, J. T., Mason, G. M., Shea, M. A., Strong, K. T., Wolf, R. A., Kelley, M. C., Hagan, M. E., Hudson, M. K., Ness, N. F., and Tascione, T. F.: *Radiation and the Space Station*, National Academy Press, Washington, D. C., 1–76, 2000.
- Smart, D. F. and Shea, M. A.: Galactic cosmic radiation and solar energetic particles, in: *Handbook of Geophysics and the Space Environment*, (Ed) Jursa, A. S., Air Force Geophysics Laboratory, 6-1–6-29, 1985.
- Smart, D. F. and Shea, M. A.: Geomagnetic cutoffs: a review for space dosimetry applications, *Adv. Space Res.*, 14(10), 787–796, 1994.
- Smart, D. F. and Shea, M. A.: World grid of calculated cosmic ray vertical cutoff rigidities for epoch 1990.0, 25th ICRC Proc., 2, 401–404, 1997a.
- Smart, D. F. and Shea, M. A.: Calculated cosmic ray cutoff rigidities at 450 km for epoch 1990.0, 25th ICRC Proc., 2, 397–400, 1997b.
- Smart, D. F., Shea, M. A., and Flückiger, E. O.: Calculated vertical cutoff rigidities for the International Space Station during magnetically quiet times, 26th ICRC Proc., 7, 394–397, 1999a.
- Smart, D. F., Shea, M. A., Flückiger, E. O., Tylka, A. J., and Boberg, P. R.: Calculated vertical cutoff rigidities for the International Space Station during magnetically active times, 26th ICRC Proc., 7, 398–401, 1999b.
- Smart, D. F., Shea, M. A., Flückiger, E. O., Tylka, A. J., and Boberg, P. R.: Changes in calculated vertical cutoff rigidities at the altitude of the International Space Station as a function of geomagnetic activity, 26th ICRC Proc., 7, 337–340, 1999c.
- Smart, D. F., Shea, M. A., and Flückiger, E. O.: Magnetospheric models and trajectory computations, *Space Sci. Rev.*, 93, 281–308, 2000.
- Störmer, C.: *The Polar Aurora*, Oxford University Press, London, 1–403, 1955.
- Tsyganenko, N. A.: A magnetospheric magnetic field model with a warped tail current sheet, *Planet. Space Sci.*, 37, 5–20, 1989.
- Tsyganenko, N. A.: Empirical magnetic field models for the space weather program, in: *Space Weather*, (Eds) Song, P., Singer, H. J., and Siscoe, G. L., Geophysical Monograph 125, American Geophysical Union, Washington, D. C., 273–280, 2001.
- Turner, R.: What we must know about solar particle events to reduce the risk to astronauts, in: *Space Weather*, (Eds) Song, P., Singer, H. J., and Siscoe, G. L., Geophysical Monograph 125, American Geophysical Union, Washington, D. C., 39–44, 2001.
- White, R. J. and Averner, M.: Humans in space, *Nature*, 409, 1115–1118, 2001.